Doping Asymmetry of a 3-orbital CuO_2 Hubbard Model

Steven R. White

University of California, Irvine, Irvine, CA 92697, USA

D.J. Scalapino

Department of Physics, University of California, Santa Barbara, CA 93106-9530, USA

While both the hole and electron doped cuprates can exhibit $d_{x^2-y^2}$-wave superconductivity, the local distribution of the doped carriers is known to be significantly different with the doped holes going primarily on the O sites while the doped electrons go on the Cu sites. Here we report the results of density-matrix-renormalization-group calculations for a three-orbital model of a CuO_2 lattice. In addition to the asymmetric dependence of the intra-unit-cell occupation of the Cu and O for hole and electron doping, we find important differences in the longer range spin and charge correlations. As expected, the pair-field response has a $d_{x^2-y^2}$-like structure for both the hole and electron doped systems.

How well does a 3-orbital Hubbard model describe the properties of the cuprates? These materials are known to be charge-transfer systems and from the analysis of Zaanan, Sawatzky and Allen[1] one would expect that a minimal model which includes a Cu $3d_{x^2-y^2}$ orbital and two O $2p\sigma$ orbitals per unit cell would be required. Indeed, early on a 3-orbital Hubbard model was proposed by several groups[2,3], and various quantum Monte Carlo[4,5] and embedded cluster calculations[6,7] have shown that this model exhibits a number of the basic magnetic and single particle spectral weight properties that are seen in the cuprates. More recently, experimental measurements of both the hole and electron doped cuprates have provided new information on the spatial charge and spin structure which can occur when these materials are doped[8–17]. So the question of whether a 3-orbital Hubbard model provides a suitable framework with which to describe the physics of the cuprates has been enlarged. Here with the experimental results for hole doped $La_{2-x}Ba_xCuO_4$ (LBCO) and electron doped $Nd_{2-x}Ce_xCuO_4$ (NCCO) in mind, we have carried out density matrix renormalization group (DMRG)[18] calculations with the goal of determining whether the 3-orbital Hubbard model

remains an adequate model for the cuprates.

Neutron scattering studies of the LTT phase of LBCO find that the doped holes form a striped structure consisting of regions with excess holes separated by π-phase shifted antiferromagnetic regions[10]. At 1/8 hole doping, superconducting correlations are observed to onset together with the stripe order[11]. This pair-density-wave phase is believed to have a d-wave pair-field which is large in the regions with excess holes and oscillates in sign between these charged regions[12,13]. Achkar et al.[14] have reported resonant soft x-ray scattering measurements which show that the charge distribution on the oxygens of LBCO have an s'-CDW orbital structure in which the charge modulations on the O_{p_x} and O_{p_y} sites in a unit cell are in phase. STM Studies of BSCCO ($p \sim 8\%$) and NaCCOC ($p \sim 12\%$) find that these materials have a predominantly d-CDW orbital form factor in which these O_{p_x} and O_{p_y} charge modulations are out of phase[15]. Finally, recent resonant x-ray scattering measurements of $Nd_{2-x}Ce_xCuO_4$ near optimal doping[16] find charge order which occurs with a similar periodicity and Cu-O bond orientation to that of the charge stripes seen in LBCO.

One-band Hubbard and t–J models have been found, within various approximations, to exhibit striped charge and spin structures[19–24], modulated nematic phases[25–27] as well as pair density wave phases[28–30]. RPA calculations for the three-band Hubbard model have also found nematic phases in certain parameter regimes[31–33]. Earlier DMRG calculations for a 3-orbital model of a two-leg CuO_2 ladder showed the expected local asymmetric charge-transfer behavior in which doped holes tend to predominantly go on the $2p\sigma$ orbitals while doped electrons go on the Cu $3d_{x^2-y^2}$ orbitals[34,35]. These calculations also found $d_{x^2-y^2}$-like pairing correlations for both hole and electron doping in which the near neighbor Cu rung and leg pair-field correlations differ in sign. Here we extend these calculations to an 8×4 CuO_2 cluster with cylindrical boundary conditions. The cylindrical boundaries reduce the edge effects associated with the ladder, more reliably representing bulk behavior. The $L \times 4$ geometry is also the minimal size that can contain stripe-like clusters of holes. With the 8×4 system we study the tendencies towards striping in the hole densities and whether doped holes or electrons modulate the phase of the antiferromagnetism. We also study the hopping kinetic energy associated with added holes or electrons, and the pairing tendencies in the doped system.

The lattice structure and the parameters of the three orbital CuO_2 model that we will study are shown in Fig. 1. The model has a CuO_2 unit cell consisting of a $3d_{x^2-y^2}$ orbital on

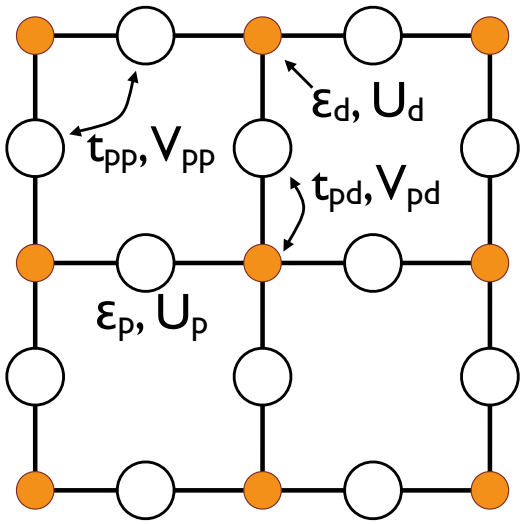

FIG. 1: The CuO_2 lattice with onsite Cu $3d_{x^2-y^2}$ and O $2p_x$ and $2p_y$ energies ϵ_d and ϵ_p, near neighbor Cu–O and O–O hoppings t_{pd} and t_{pp}, onsite Cu and O Coulomb interactions U_d and U_p and near neighbor Cu–O and O–O Coulomb interactions V_{pd} and V_{pp}, respectively. The Hamiltonian for this 3-orbital model is given in a hole representation by Eq. (1). Here we will work with energies measured in units of t_{pd}, and take as a generic set of parameters $t_{pp} = 0.5$, $\Delta_{pd} = \epsilon_p - \epsilon_d = 3$, $U_d = 8$, $U_p = 3$, $V_{pd} = 1$ and $V_{pp} = 0.75$.

the Cu site and $2p_x/2p_y$ orbitals on the x and y oxygens. In a representation in which the vacuum of the 3-orbital model has the configuration $(d^2_{x^2-y^2}p^2_x p^2_y)$, $d^+_{i\sigma}$ and $p^+_{j\sigma}$ create holes with spin σ on the i^{th} Cu and j^{th} O sites respectively, and the Hamiltonian has the form

$$\begin{aligned} H &= \Delta_{pd}\sum_{i\sigma} p^+_{i\sigma}p_{i\sigma} - t_{pd}\sum_{\langle ij\rangle\sigma}(d^+_{i\sigma}p_{j\sigma} + p^+_{j\sigma}d_{i\sigma}) \\ &- t_{pp}\sum_{\langle ij\rangle\sigma}(p^+_{i\sigma}p_{j\sigma} + p^+_{j\sigma}p_{i\sigma}) \\ &+ U_d\sum_i n^d_{i\uparrow}n^d_{i\downarrow} + U_p\sum_i n^p_{i\uparrow}n^p_{i\downarrow} \\ &+ V_{pd}\sum_{\langle ij\rangle} n^d_i n^p_j + V_{pp}\sum_{\langle ij\rangle} n^p_i n^p_j \end{aligned} \tag{1}$$

Here $\Delta_{ps} = \epsilon_p - \epsilon_d$ is the energy difference between having a hole on an O site versus a Cu site, t_{pd} and t_{pp} are one-hole hopping matrix elements between near-neighbor Cu and O sites and near-neighbor O sites, respectively. The sums $\langle ij\rangle$ in Eq. 1 denote sums over the relevant nearest-neighbor sites. U_d and U_p are the onsite Cu and O Coulomb interactions and V_{pd} and V_{pp} are the nearest-neighbor Cu–O and O–O Coulomb interactions, respectively. The phases of the orbitals have been fixed such that the signs of the hopping matrix elements

remain the same throughout the lattice and are positive.

The hopping parameters t_{pd} and t_{pp} found for La_2CuO_4 and Nb_2CuO_4 in various cluster and LDA calculations are relatively close to each other. We will measure energies in units of t_{pd} and set $t_{pp}/t_{pd} = 0.5$ for both of these materials[9,36]. The primary difference in the one-electron parameters occurs in Δ_{pd} where the absence of the apical oxygens in Nd_2CuO_4 is expected to lead to a reduction in Δ_{pd} relative to La_2CuO_4. Indeed this is found in LDA calculations, however the appropriate bare values of Δ_{pd} to use in the 3-orbital Hamiltonian Eq. (1) has posed a problem because of double counting corrections[6,37]. Here we find that setting $\Delta_{pd}/t_{pd} = 3$ gives reasonable values for the charge gap and exchange interaction. Thus, working in units of t_{pd} we will take for a canonical set of parameters

$$t_{pp} = 0.5,\ \Delta_{pd} = \varepsilon_p - \varepsilon_d = 3,\ U_d = 8,\ U_p = 3,\ V_{pd} = 1,\ V_{pp} = 0.75 \tag{2}$$

These parameters are appropriate for a charge transfer system for which $U_d > \varepsilon_p - \varepsilon_d = \Delta_{pd}$ and $\Delta_{pd} > 2t_{pd}$. Using a similar set of parameters for a 2-leg CuO_2 ladder we previously found at half-filling a charge gap $\Delta_c \sim t_{pd}$ and a spin gap $\Delta_s \sim 0.03 t_{pd}$. For a 2-leg ladder the effective exchange coupling $J \sim 2\Delta_s \sim 0.06 t_{pd}$. For t_{pd} of order 1 to 2 eV, these correspond to reasonable values for the charge gap and the exchange interaction. Our plan is to use this same set of parameters for both the hole and electron doped systems and focus on the differences that arise between them. We will comment on the effect of reducing t_{pp} and, for the electron doped case, the effect of reducing Δ_{pd}.

The DMRG calculations will be carried out for an 8×4 CuO_2 lattice which has periodic boundary conditions in the 4-unit cell y-direction and open ends in the 8-unit cell x-direction. For the charge and spin studies, we will work with a fixed number of holes $32 + N$ and a hole density per CuO_2 unit cell $x = 1 + N/32$ which is 1 for the undoped system. Positive values of N ($x > 1$) correspond to hole doping and negative values of N ($x < 1$) to electron doping. We typically did 15 DMRG sweeps, keeping up to $m = 4000$ states on the last sweep. This led to excellent convergence for the local quantities that we report here. A typical maximum truncation error was $\sim 10^{-5}$; extrapolating the truncation error to zero gave typical fractional errors in the total energy also about $\sim 10^{-5}$. Without extrapolation, fractional errors in energy were estimated to be less than 10^{-4}, and absolute errors in local quantities were in the range $10^{-3} - 10^{-4}$. The good overall convergence for this cluster suggests that wider systems, say up to width 6, will be accessible for near-future studies.

In Fig. 2 we show the effect of doping on the local charge density and squared spin moments on the Cu and O sites as a function of the hole density x. As we will discuss later, there can be inter- and intra-cell spatial structure in the charge and spin. The results shown in Fig. 2 represent site averages taken over the 8×4 lattice. For the undoped $x = 1$ ($N = 0$) system where there is one hole per CuO_2 unit cell, Fig. 2 shows that the hole occupation is approximately 80% on the Cu site and 10% on each of the two O sites for the parameters that we have chosen. When additional holes are added they go approximately 75% onto the two O sites and 25% onto the Cu site of the unit cell. Alternatively, under electron doping, the added electrons go approximately 90% onto the Cu site and only 10% onto the two O sites. This is of course what one would expect for a charge-transfer system. The change in the square of the spin moments on the Cu and O sites is seen to vary with the hole concentration x in a similar manner to that of the charge occupation. For electron doping ($x < 1$), an electron added to a Cu site removes the hole spin moment leading to a decrease in $\langle S^2 \rangle$ averaged over the lattice, while for hole doping the square of the O hole spin moment increases as holes are primarily added to the O sites.

To study the longer range spin and charge correlations, we have applied a weak staggered magnetic field to the Cu sites on the left hand edge of the 8×4 lattice. The expected antiferromagnetic response of the undoped system is shown in Fig. 3. Here, the diameters of the circles are proportional to the density of the holes and the lengths of the arrows are proportional to the spin moments. One sees, as shown in Fig. 2 that the holes are mainly on the Cu sites. The applied edge field has broken the spin symmetry and there is a well formed antiferromagnetic spin pattern.

In Fig. 4 we contrast the results for hole doping on the left with electron doping on the right. In this figure, the hole density distribution of the undoped lattice shown in Fig. 3 has been subtracted. The diameters of the circles for hole doping on the left are proportional to the added hole density while the diameters of the circles on the right are proportional to the added electron density. In this figure the diameter scale used for the hole density is 0.1 and for the electron density 0.15. In the top left hand lattice shown in Fig. 4, 2 holes have been added to the 32 holes of the undoped 8×4 lattice giving $x = 1.0625$. The lattices shown below this have 4,6 and 8 holes added corresponding to hole concentrations x per CuO_2 unit cell of 1.125, 1.1875 and 1.25, respectively. The lattices on the right hand side of Fig. 4 show similar results for the case in which electrons are added (or holes removed).

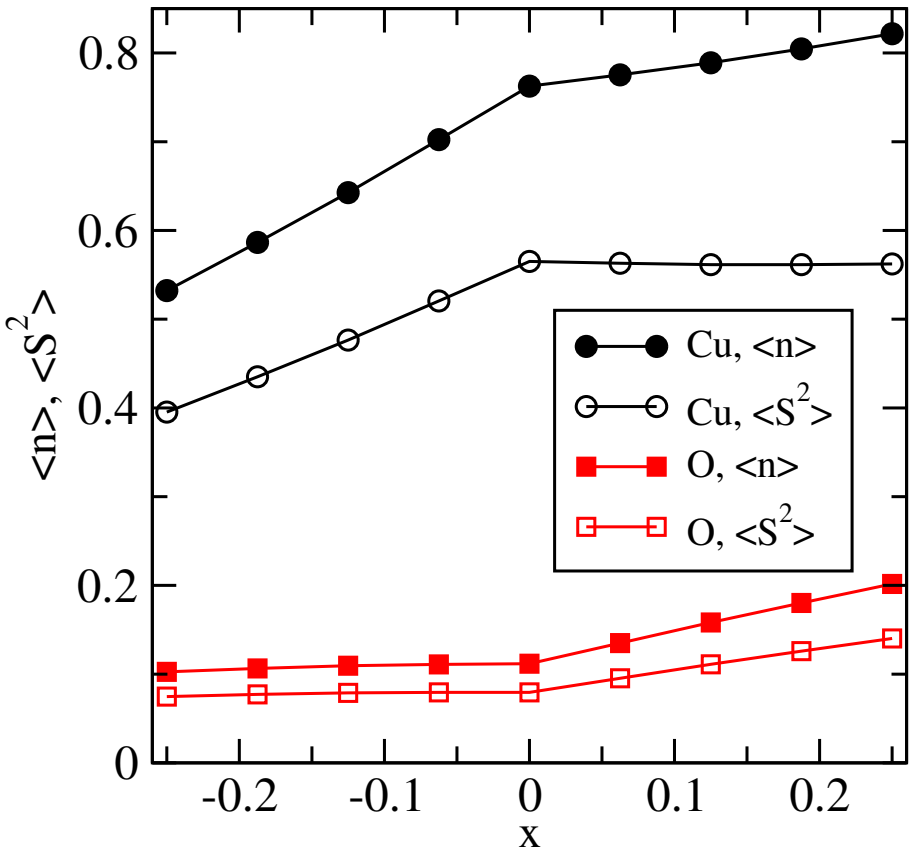

FIG. 2: The hole density $\langle n \rangle$ and the square of the spin moment $\langle S^2 \rangle = \frac{3}{4}\langle n_\uparrow + n_\downarrow - 2n_\uparrow n_\downarrow \rangle$ on the Cu (black circles) and O (red squares) sites versus the hole density $x = 1 + N/32$ per CuO_2 unit cell. The undoped 8×4 CuO_2 lattice has 32 holes and $x = 1$. $N > 0$ ($x > 1$) corresponds to doping additional holes while $N < 0$ ($x < 1$) corresponds to electron doping which reduces the number of holes.

From top to bottom these lattices have 30, 28, 26 and 24 holes, respectively, corresponding to $x = 0.9375$, 0.875, 0.8125 and 0.75. As in Fig. 3, a staggered magnetic field ($h = 0.1$) was applied to the Cu sites on the left-hand edge of the lattice.

As shown in Fig. 2, the additional holes tend on average to go onto the O sites, but as seen in Fig. 4 their distribution is not uniform. For hole doping there is a tendency for stripe formation separated by π-phase shifts in the antiferromagnetic correlations. For $x = 1.125$ there are two, approximately Cu-site centered, stripes separated by a π-phase shifted antiferromagnetic region similar to the well known behavior of $La_{1.48}Nd_{0.4}Sr_{0.12}CuO_4$[10]. For $x = 1.0625$ there is a single stripe and for $x = 1.1875$, corresponding to the addition of 6 holes on the 8×4 lattice, one can see the remnants of a three stripe structure. This structure

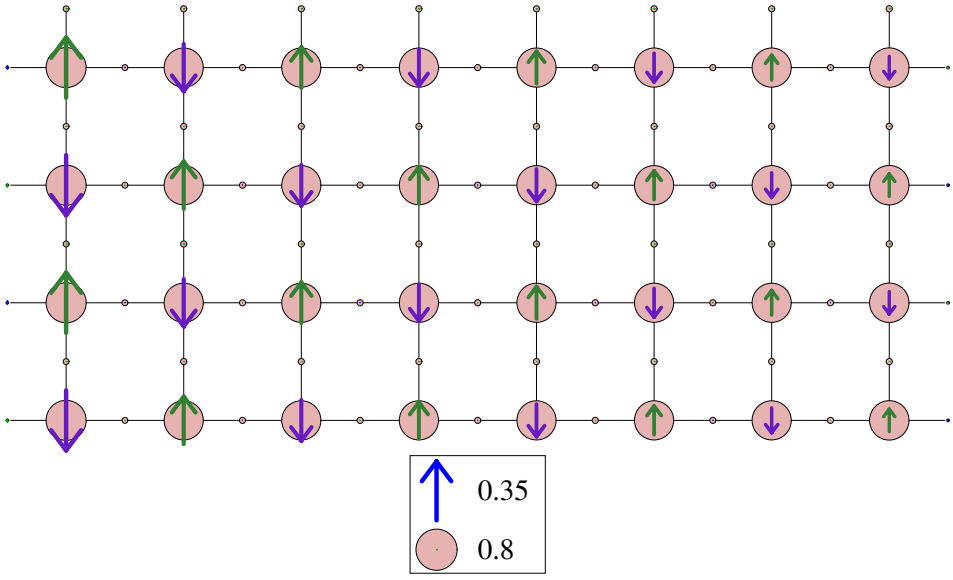

FIG. 3: The hole occupation $\langle n \rangle$ and spin structure $\langle S_z \rangle$ for the undoped (32 hole) 8×4 CuO_2 lattice. The hole occupation is proportional to the diameter of the circles. A staggered magnetic field of magnitude $h = 0.1$ was applied to the Cu sites along the left-hand edge of the 8×4 CuO_2 lattice which has periodic boundary conditions in the y direction and open end boundary conditions in the x-direction.

vanishes for the strongly overdoped $x = 1.25$ case. The stripe spacing for the three lower hole dopings is consistent with the relation $d^{-1} = 2(x-1)$ and the well known spin $\delta_{\rm spin}$ and charge $\delta_{\rm charge}$ incommensurability relation $\delta_{\rm charge} = 2\delta_{\rm spin}$ found in the La-based cuprates[8,10]. A closer look at the structure of the charge and spin distributions for the 1/8 ($x = 1.125$) hole doped lattice is shown in Fig. 5(a). Here a weak staggered magnetic field has been applied to both ends of the 8×4 lattice. In this case, the $x = 1.125$ hole doped system exhibits bond centered charged stripes separated by π-phase shifted antiferromagnetic regions. The charge modulations on the O_{p_x} and O_{p_y} sites are in phase leading to what was called an s'–CDW–SDW phase in Ref. 14. There may be an additional small admixture of d-CDW. Of course the 8×4 lattice already breaks C4 symmetry so one expects differences in the x and y oxygen hole occupations. Increasing V_{pp} leads to an increase in these differences[38] but the s' symmetry remains dominant.

For the electron doped system, one sees on the right hand side of Fig. 4 that the spin and charge structure appears quite different from the hole doped case. Of course the doped

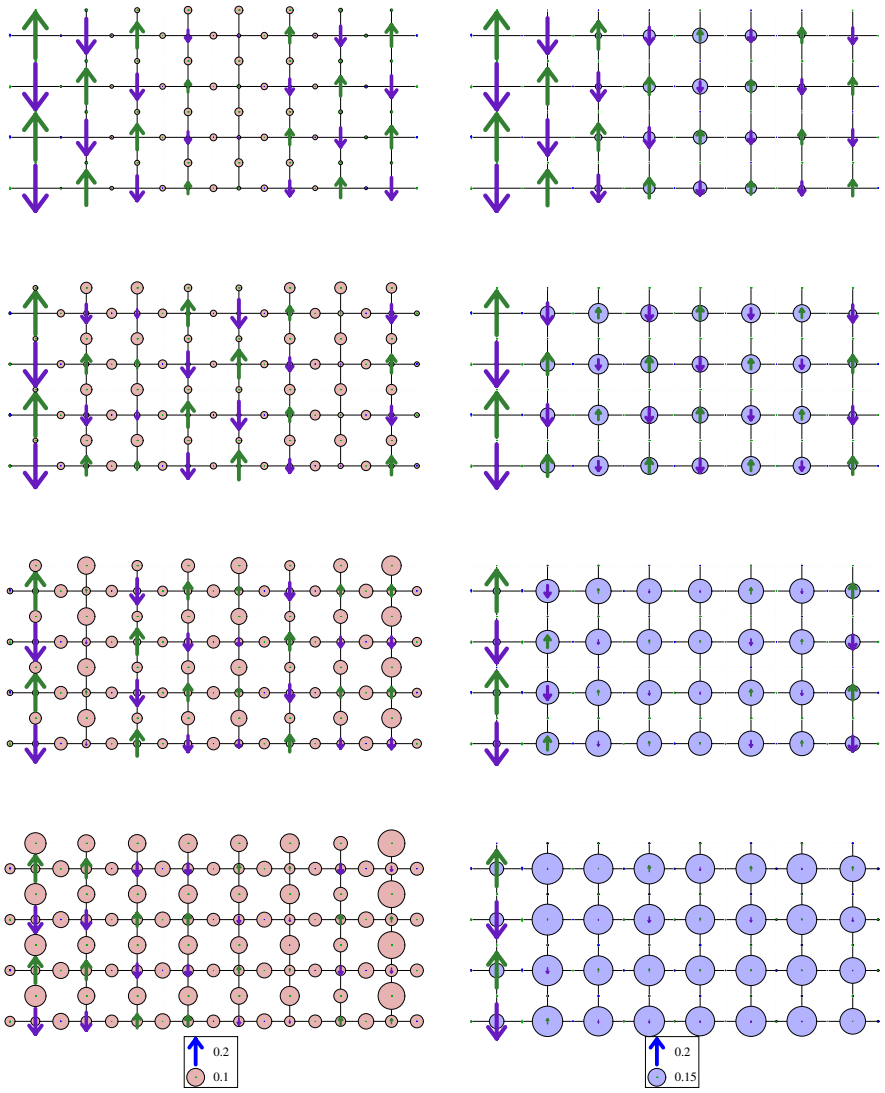

FIG. 4: Charge and spin structure for the hole (left) and electron (right) doped lattices for the parameters given in Eq. (2). Here the hole density distribution for the undoped lattice shown in Fig. 3 has been subtracted. The added hole density on a site is proportional to the diameter of the red circles shown on the left. Similarly, the diameter of the blue circles on the right is proportional to the added electron density. Note the difference in the diameter scales for the hole and electron doped figures. The small $\sim 5\%$ of the additional electron density that goes onto an O site is not visible on this scale. For the 8×4 lattice, the left hand figures (top to bottom) correspond to the addition of 2,4,6 and 8 holes respectively, while the right hand figures correspond to the addition of a corresponding number of electrons. A staggered magnetic field of magnitude $h = 0.1$ has been applied to the Cu sites on the left-hand edge of the lattice.

electrons go dominantly on to the Cu sites and initially the small concentration of added electrons are repelled from the open edge boundaries by the "infinite" edge potential. However, for these parameters, by the time the electron doping reaches 0.125, a relatively uniform density of the added electrons is spread over the Cu sites and the antiferromagnetic order remains. A closer look at the 1/8 electron doped lattice is shown in Fig. 5(b). Here one can see that there are two charge stripes but the antiferromagnetic correlations remain commensurate. Thus for these parameters we find charge stripes with incommensurate antiferromagnetism for hole doping and commensurate antiferromagnetic spin correlations for electron doping. This remains the case for the electron doped system when Δ_{pd} is reduced as is expected in the T' structure where the apical oxygens are absent. Another important parameter is t_{pp} which determines the effective hopping t' between next-near neighbor Cu sites. In Hubbard and $t-t'-J$ models it is known that t' affects the stripe stability[12,24]. Here we find that when the oxygen-oxygen hopping t_{pp} is reduced, the amplitude of the charge stripes is increased and the spin structure for the electron doped system also becomes incommensurate as shown in Fig. 5(c) for $t_{pp}=0$. The effect of reducing t_{pp} acts to increase the frustration associated with the antiferromagnetic background and gives rise to the π-phase shifted antiferromagnetic regions separating the charge stripes. We find that when t_{pp} is reduced (below $\lesssim 0.25$), striping can occur for both the electron and hole doped system. However, the tendency for striping is stronger in the hole doped system.

The addition of holes to the filled band vacuum configuration ($d^2_{x^2-y^2}p^2_x p^2_y$) lowers the kinetic energy. For the hole Hamiltonian, Eq. (1), with positive hopping parameters this means that one expects the Cu-O and O-O hole hopping strengths $\sum_s \langle d^+_{is}p_{js} + p^+_{js}d_{is}\rangle$ and $\sum_s \langle p^+_{is}p_{js} + p^+_{js}p_{is}\rangle$ to be positive for the 32 hole doped system as illustrated in Fig. 6(a).

The Cu-O hopping strength is larger than the O-O hopping strength reflecting the fact that the doped holes are of order 80% on the Cu sites. When additional holes are added, the hopping strength increases further. The difference in the hopping strengths between the 36 hole doped lattice and the undoped 32 hole lattice are illustrated in Fig. 6(b). In the case of hole doping, the holes are distributed to both the Cu and O sites ($\sim 25\%$ to the Cu and $\sim 37.5\%$ to each of the O sites) leading to the enhancement of both the Cu-O and O-O hopping strengths shown in Fig. 6(b). In addition, one sees evidence of the charge stripe structure.

For the case of electron doping, the electrons go dominantly on the Cu sites. This

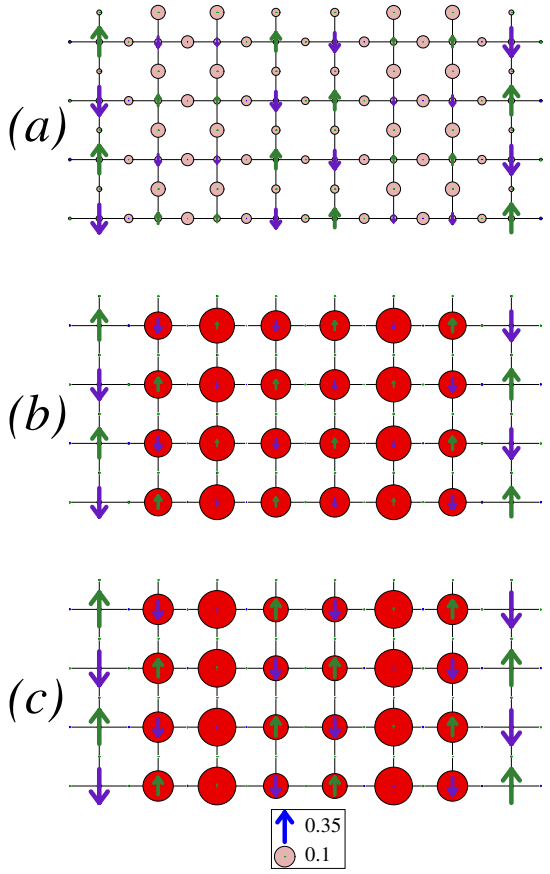

FIG. 5: (a) The charge and spin structure of the 1/8 ($x = 1.125$) hole doped system with a weak staggered magnetic field $h = 0.1$ applied to both ends of the 8×4 lattice. Here an s'-CDW–SDW structure is seen. (b) The charge and spin structure of the 1/8 ($x = 0.875$) electron doped system with $t_{pp} = 0.5$. Here we find only a weak charge modulation and a commensurate spin antiferromagnetic structure. (c) Similar to the $x = 0.875$ electron doped system shown in (b) but with $t_{pp} = 0.0$. In this case there is an incommensurate antiferromagnetic spin structure similar to that of the hole doped system.

reduction of the average number of holes on the Cu sites leads to the reduction in the Cu-O hole hopping strength as shown in Fig. 6(c). Although the reduction of the average hole occupation on each O is only of order 5%, one might have expected that this would also reduce the strength of the O-O hole hopping. However, as shown in Fig. 6(c), the O-O hopping strength is in fact slightly increased. The overall change in hopping strength is significantly smaller for the electron doped system. The total change in the kinetic energy measured in units of t_{pd} per added hole is of order -3.2 while per added electron it is only

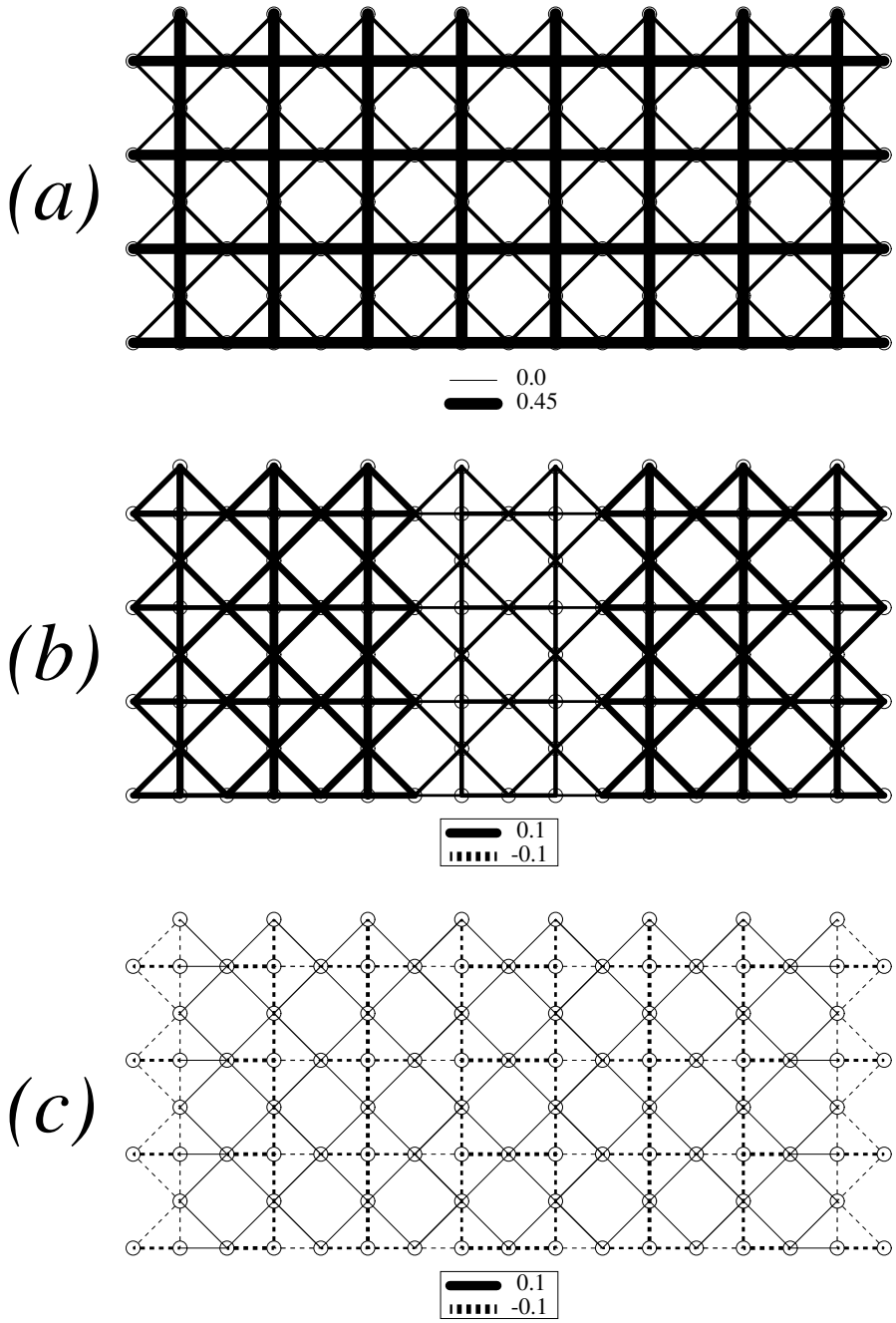

FIG. 6: (a) The hopping strength on each bond for the undoped system. (b) The difference in the hopping strength relative to the undoped system for the hole doped system with $x = 1.125$. (c) The same as (b), but for the electron doped system, $x = 0.875$

+0.7. This is consistent with the notion that the doped holes will enter a region of the band between Γ and M where there is significant dispersion while the electrons will enter near X where the dispersion is flat.

In order to study the pairing response, we have applied a proximity singlet pair-field that couples to near neighbor Cu sites along the x direction,

$$\frac{\Delta_0}{2} \sum_{(\ell_x,\ell_y)} \left(\Delta_x^+(\ell_x,\ell_y) + \Delta_x(\ell_x,\ell_y) \right) \tag{3}$$

with $\Delta_x(\ell_x,\ell_y) = \left(d_{\ell_x+1,\ell_y\uparrow} d_{\ell_x,\ell_y\downarrow} - d_{\ell_x+1,\ell_y\downarrow} d_{\ell_x,\ell_y\uparrow} \right)/\sqrt{2}$. The Cu-O near neighbor responses in the x-direction $\langle \Delta_x(\ell_x,\ell_y) + \Delta_x^+(\ell_x,\ell_y) \rangle/2$ has a negative sign and is shown as the dashed lines in Fig. 7. The solid lines, which indicate a positive value, show the pair-field response $\langle \Delta_y(\ell_x,\ell_y) + \Delta_y^+(\ell_x,\ell_y) \rangle/2$ between near neighbor Cu-O sites in the y direction. For these calculations the average hole number was set by a chemical potential μ. In the top panel, Fig. 7(a), $\mu = -1.0$, giving an average hole number $\langle N \rangle = 36.05$ ($x \sim 1.125$) while for the lower panel, Fig. 7(b), $\mu = -3.2$ giving $\langle N \rangle = 28.14$ ($x \sim 0.875$). Both the hole doped pair-field response shown in Fig. 7(a) and the electron doped case shown in Fig. 7(b) have the expected d-wave-like sign change.

If the proximity pair-field is applied only between the horizontal Cu-Cu sites on the left edge of the lattice, the induced pair-field decays rapidly in the x-direction for the hole doped system and somewhat more slowly for the electron doped case. The longer range pair-field correlations are suppressed by finite size effects. These are particularly severe for the periodic in y (tube-like) geometry of our CuO_2 lattice. As seen in Fig. 4 for the hole doped lattice, a stripe appears each time a pair of holes is added for 2, 4 and 6 holes. This is consistent with previous 2-leg ladder studies where it was found that the preferred filling was 2 holes per 4 rungs[23,24]. Thus for an 8×4 CuO_2 tube a low-energy fluctuation of ± 2 holes involves the creation or destruction of a stripe, leading to a high energy spin configuration with a domain wall without holes. Alternatively, one could consider a configuration which has 4 holes in a stripe, but this is also energetically unfavorable. While this effect is less severe for the electron doped system shown in Fig. 7(b) and the pair-field response is stronger because it lacks the antiferromagnetic domain walls, we expect that the small 8×4 size of the lattice still acts to suppress the hole number fluctuations. Properly comparing the pairing between the electron doped and hole doped systems will require larger systems, and if there are stripes they should be long, running lengthwise down the cylinder, either horizontally or

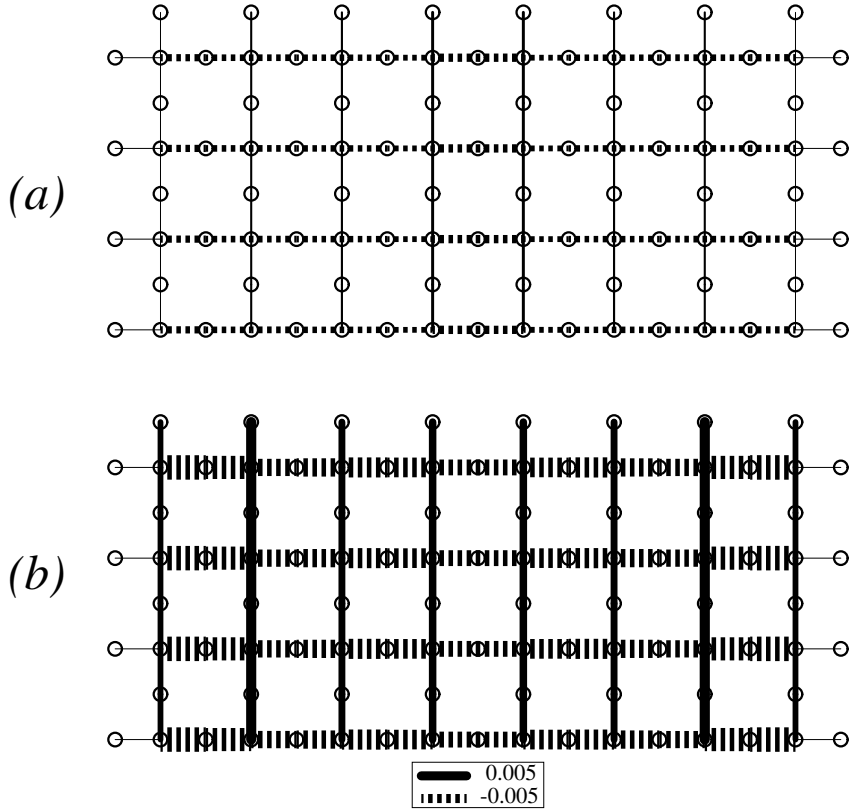

FIG. 7: The pair-field induced by the proximity pair-field, Eq. (3), for the hole $x \approx 1.125$ (a) and electron $x \approx 0.875$ (b) doped systems. Here the dashed lines denote a negative pair-field amplitude between near neighbor Cu-O pairs of sites while the solid lines denote a positive pair-field amplitude. The applied proximity pair-field is between near neighbor Cu-Cu pairs of sites in the x-direction with magnitude $\Delta_0 = 0.2$, and the response shows the expected $d_{x^2-y^2}$-like behavior for both the hole and electron doped systems.

spiraling.

In summary, we have studied an 8×4 three orbital Hubbard model for CuO_2 with parameters chosen to give a realistic charge gap and exchange coupling. With one hole per CuO_2 unit, the hole occupation is approximately 80% on the Cu $d_{x^2-y^2}$ orbital and in the presence of a weak staggered edge magnetic field commensurate antiferromagnetic correlations are found to extend across the lattice. When additional holes are added they go $\sim 75\%$ onto the O sites and charge stripes separated by π-phase shifted antiferromagnetic regions appear. The O hole occupation and the Cu spin structure has an s'-CDW-SDW

like structure[14]. When additional electrons are added, they go approximately 90% onto the Cu $d_{x^2-y^2}$ orbitals. For our small cluster, there is a weak tendency for charge modulations but the antiferromagnetic spin correlations remain commensurate. However, when the oxygen-oxygen one electron hopping t_{pp} is reduced, a clear striped structure appears with incommensurate antiferromagnetic correlations. For both the hole and electron doped systems, the response of the y-near-neighbor Cu-Cu pair-field is out of phase (d-wave like) with respect to the x-near neighbor Cu-Cu pair-field induced by an applied x-near-neighbor proximity pair-field. These pair-field correlations are short range reflecting the finite size and geometric restrictions of the CuO_2 cluster studied.

We would like to thank J.C.S. Davis, S.A. Kivelson, M.A. Metlitski, S. Sachdev and J.M. Tranquada for insightful discussions. SRW acknowledges support from the NSF under grant DMR-1161348 and from the Simons Foundation through the Many Electron collaboration. DJS acknowledges the support of the Center for Nanophase Materials Science at ORNL, which is sponsored by the Division of Scientific User Facilities, U.S. DOE.

---

[1] J. Zaanen, G. A. Sawatzky, and J.W. Allen, *Phys. Rev. Lett.* **55**, 418 (1985).

[2] V.J. Emery, *Phys. Rev. Lett.* **58**, 2794 (1987).

[3] C.M. Varma, S. Schmitt-Rink, E. Abrahams, *Solid State Comm* **62**, 681 (1987).

[4] G. Dopf, A. Muramatsu, and W. Hanke, *Phys Rev B* **41** 9264 (1990).

[5] R. T. Scalettar, D. J. Scalapino, R. L. Sugar, and S. R. White, *Phys Rev B* **44** 770 (1991).

[6] P.R.C. Kent, T. Saha-Dasgupta, O. Jepsen, O.K. Andersen, A. Macridin, T.A. Maier, M. Jarrell, and T.C. Schulthess, *Phys. Rev. B* **78**, 035132 (2008).

[7] E. Arrigoni, M. Aichhorn, M. Daghofer and W. Hanke, *New J. Physics* **11**, 055066 (2009).

[8] John M. Tranquada, *AIP Conf. Proc.* **1550**, 114–187 (2013).

[9] N.P. Armitage et al., *Rev. Mod. Phys.* **82**, 2421–2487 (2010).

[10] M. Fujita et al., *Phys Rev B* **70** 104517 (2004).

[11] Q. Li, M. Hücker, G.D. Gu, A.M. Tsvelik, and J.M. Tranquada, *Phys. Rev. Lett.* **99**, 067001 (2007).

[12] A. Himeda, T. Kato, and M. Ogata, *Phys. Rev. Lett.* **88**, 117001 (2002).

[13] E. Berg, E. Fradkin, E.-A. Kim, S.A. Kivelson, V. Oganesyan, J.M. Tranquada, and S.C. Zhang,

Phys. Rev. Lett. **99**, 127003 (2007).

[14] A.J. Achkar, F. He, R. Sutarto, Christopher McMahon, M. Zwiebler, M. Hucker, G.D. Gu, Ruixing Liang, D.A. Bonn, W.N. Hardy, J. Geck, D.G. Hawthorn, arXiv:1409.6787.

[15] K. Fujita, M.H. Hamidian, S.D. Edkins, Chung Koo Kim, Y. Kohsaka, M. Azuma, M. Takano, H. Takagi, H. Eisaki, S. Uchida, A. Allais, M.J. Lawler, E.-A. Kim, Subir Sachdev, J.C. Séamus Davis, *Proceedings of the National Academy of Sciences of the USA* **111**, E3026-E3032 (2014).

[16] Eduardo H. da Silva Neto, Riccardo Comin, Feizhou He, Ronny Sutarto, Yeping Jiang, Richard L. Greene, George A. Sawatzky, and Andrea Damascelli. arXiv:1410.2253.

[17] R. Comin et al. , arXiv 1402.5415.

[18] S.R. White, *Phys. Rev. Lett.* **69**, 2863 (1992); *Phys. Rev. B* **48**, 10345 (1993).

[19] D. Poilblanc and T.M. Rice, *Phys. Rev. B* **39**, 9749 (1989).

[20] J. Zaanen and O. Gunnarsson, *Phys. Rev. B* **40**, 7391 (1989).

[21] K. Machida, *Physica C: Superconductivity* **158**, 192 (1989).

[22] H. Schulz, *Journal de Physique* **50**, 17 (1989).

[23] S.R. White and D.J. Scalapino, *Phys. Rev. Lett.* **80**, 1272 (1998).

[24] S.R. White and D.J. Scalapino, *Phys. Rev. B* **60**, R753 (1999).

[25] M.A. Metlitski and S. Sachdev, *New J. Phys.* **12**, 105007 (2010); A. Thomson and S. Sachdev, arXiv 1410.3483.

[26] Jay Deep Sau and Subir Sachdev, *Phys. Rev. B* **89**, 075129 (2014).

[27] M. H. Fischer, S.Wu, M. Lawler, A. Paramakanti, and Eun-Ah Kim, New Journal of Physics 16, 093057 (2014).

[28] Erez Berg, Eduardo Fradkin, Steven A. Kivelson, John Tranquada, *New J. Phys* **11**, 115004 (2009).

[29] Philippe Corboz, T.M. Rice, Matthias Troyer, *Phys. Rev. Lett.* **113**, 046402 (2014).

[30] Eduardo Fradkin, Steven A. Kivelson, John M. Tranquada, arXiv:1407.4480.

[31] S. Bulut, W.A. Atkinson and A.P. Kampf, *Phys. Rev. B* **88**, 155132 (2013).

[32] W.A. Atkinson, A.P. Kampf and S. Bulut, arXiv 1404.1335.

[33] T.A. Maier, D.J. Scalapino, arXiv 1405.5238.

[34] E. Jeckelmann, D.J. Scalapino, and S. R. White Phys. Rev. B 58, 9492 (1998).

[35] S. Nishimoto, E. Jeckelmann, and D.J. Scalapino Phys. Rev. B 66, 245109 (2002).

[36] K. Haule, T. Birol and G. Kotliar, arXiv:1310.1158 (2013).

[37] M.S. Hybertsen, M. Schluter, and N.E. Christensen, *Phys. Rev. B* **39**, 9028 (1989).

[38] S.A. Kivelson, E. Fradkin and T. Geballe, *Phys. Rev. B* **69**, 144505 (2014).